Article

Cite This: *Biomacromolecules* XXXX, XXX, XXX–XXX

pubs.acs.org/Biomac

Enzyme-Lignin Nanocapsules Are Sustainable Catalysts and Vehicles for the Preparation of Unique Polyvalent Bioinks

Eliana Capecchi,[†] Davide Piccinino,[†] Bruno Mattia Bizzarri,[†] Daniele Avitabile,[‡] Claudia Pelosi,[§] Claudia Colantonio,[§] Giuseppe Calabrò,[§] and Raffaele Saladino*[,†]

[†]Department of Biological and Ecological Sciences (DEB), Tuscia University, Via S. Camillo de Lellis snc, 01100 Viterbo, Italy

[‡]IDI Farmaceutici srl, Via dei Castelli Romani 83/85, Pomezia, 00040 Rome, Italy

[§]Department of Economics, Engineering, Society and Business Organization (DEIM), Tuscia University, 01100 Viterbo, Italy

Supporting Information

ABSTRACT: Reactive lignin nanocapsules catalyze a pigmentation reaction to furnish an innovative type of sustainable polyvalent bioink. In this nanodevice, the pigment, vehicle, binder, and additive are included in a single confined spherical space. Bioinks with different shades of color, black, gray, yellow-like, pink-like, and red/brown hues, have been prepared by selecting the reactants and the pigmentation process. Lignin nanocapsules play multiple functions in the support and activation of the enzyme necessary for the synthesis of pigments. Lignin nanocapsules protected the melanin pigment from alkaline and UV-degradation treatment.

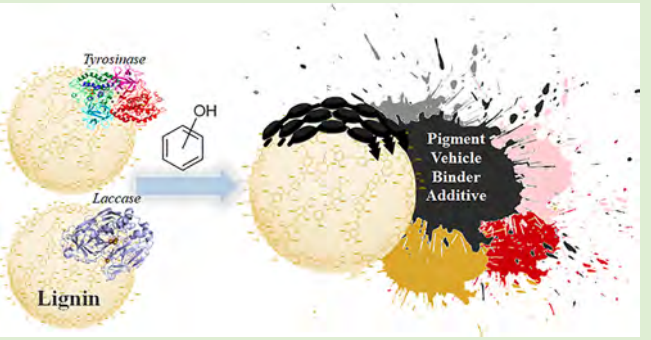

INTRODUCTION

Over the past several years, increased legislative attention and safety burden, as well as environmental concerns, oriented traditional printing ink formulations toward the use of renewable resources with reduced or absent environmental impact.[1] Bioinks might not only limit dependency on fuel-oil, but they also can drive the development of novel technological applications.[2] Ink formulations are usually composed of four type of ingredients, namely, pigment, vehicle and binder, additive, and solvent.[3] Moreover, depending on the specific application and on the viscosity of the binder, no additional solvent might be necessary, leading to solvent-free ink.[4] Water can be used as a sustainable solvent in environmental friendly ink formulations.[5] Tall oil rosin (colophony),[6] soybean, and edible vegetable oils,[7] frying oils,[8] karanja oil,[9] abietic acid polymers,[10] and polysaccharides[11] have all been used as binders to replace fuel-oil-derived synthetic materials. Unfortunately, drawbacks are envisaged in the application of these biobinders, since they are in competition with food production, demanding toxic additives to improve rheological properties.[12]

Lignin, the main byproduct of the pulp and paper industry and of biorefinery processes, is a sustainable binder due to its favorable physical-chemical properties associated with low cost and easy availability.[13] Lignin is a highly branched polyphenolic polyether consisting of oligomeric subunits produced by radical polymerization of monolignols, *para*-coumaryl alcohol, coniferyl alcohol, and sinapyl alcohol.[14] This polymer shows antioxidant activity,[15−18] UV-shielding protection,[19−21] anticorrosion effects,[22,23] and electrochemical responsiveness.[24−26] Amine salts of the Kraft lignin are additives in water-based pigments, acting both as grinding agents for the pigment in the formulation, and as a binder in the printing processes.[27] Moreover, organosolv lignin (OL) has been applied as a filler in different ink formulations, improving the viscosity of the medium,[28] as well as in sustainable formaldehyde resins.[29] In a similar way, nitrate alkaline lignin esters,[30] carboxylate softwood lignin,[31] and acetylated lignin[32] have been used as binders in ink formulations. Nanoparticles and nanocapsules of lignin showed innovative pharmaceutical and technological applications.[33−35] Nanoscaled binders are of relevant interest, since they can penetrate easily into the structure of bulky paper, promoting the rate of biodegradation.[36] For this reason, submicron Kraft lignin particles have been applied as binders in novel water ink formulations.[37] The main advantage of lignin nanodevices resides in the high biocompatibility, in the possibility to be degraded by microorganisms, and in the emergence of novel scale-dimensional chemical and physical properties.[38]

Improved UV-shielding properties and antioxidant activities emerged during the preparation of OL and lignosulfonate nanocapsules by a template layer-by-layer (LbL) approach,[39] consisting on the alternative deposition of polyelectrolytes of different electrical charge.[40] Lignin nanodevices have been used as a support for the immobilization of enzymes,[41]

Received: February 8, 2019
Revised: March 29, 2019
Published: March 29, 2019

DOI: 10.1021/acs.biomac.9b00198
Biomacromolecules XXXX, XXX, XXX–XXX

including tyrosinase and laccase.[42] In this latter case, they showed capacity to improve the enzymatic activity by the boosting effect[43] and by direct and mediated electron transfer processes.[44] Tyrosinase and laccase catalyze the preparation of several pigments and dyes under natural or synthetic procedures.[45] Thus, lignin nanocapsules functionalized with oxidative enzymes can perform as biocatalyst for the synthesis of the pigment and as vehicle, binder, and additive for the newly synthesized pigment. Here we describe the use of lignin nanocapsules loaded with tyrosinase from *Aspergillus niger* and, in alternative, with laccase from *Trametes versicolor*, for the efficient "in situ" polymerization of appropriate chemical precursors to afford a large panel of pigments. The pigments resulted to be stably linked to the support, affording a large panel of colored nanocapsules to be used as an unique polyvalent bioink.

EXPERIMENTAL PART

Materials. OL was purchased from Chemical Point (Oberhaching, Germany). Tyrosinase from *Aspergillus niger* (1000 U/mg), laccase from *Trametes versicolor* (1.07 U/mg), Bradford reagent, poly-(diallyldimethylammonium chloride) (PDDA, 20%v/v water solution), chitosan (CH, low molecular weight) with 20% chitin units, melanin, 2,2-azinobis(3-ethylbenzothiazoline-6-sulfonic acid) (ABTS), L-tyrosine, L-3,4-dihydroxyphenylalanine (L-DOPA), epicatechin, catechol, 4-amino benzoic acid, hydroquinone, 3-aminobenzoic acid, resorcinol, and *para*-phenylenediamine were purchased from Sigma−Aldrich (St. Louis, MO, USA) and were used without any further purification. All experiments were repeated in triplicate using native and immobilized tyrosinase or laccase in phosphate buffer saline (PBS 0.1 M pH 7) or sodium acetate buffer (Na-acetate buffer 0.1 M pH 5), respectively. Solutions were prepared using Milli-Q water (ρ = 18.2 MΩ cm a 25 °C; TOC < 10 μg L^{-1}; Millipore, Molsheim, France).

Preparation of Nanocapsules by a Template-Based LbL Procedure. Nanocapsules were prepared by applying a modified version of the LbL procedure using OL as the template.[46] Briefly, commercially available OL (20 mg) was dissolved in THF (20 mL), followed by filtration (0.45 μm syringe filter) and dialysis against deionized water, for 24 h at 25 °C. The suspension (15 mL) of OL nanocapsules in Milli-Q water (1 mg/mL; pH 4.2) was added dropwise to PDDA or CH solution (1.0 mg/mL, Milli-Q water) under slow magnetic stirring.[47] After 2 h, the final suspension was centrifuged (6000 rpm, 20 min), and the supernatant removed. The nanocapsules were rinsed with deionized water, recovered by centrifugation (6000 rpm, 20 min) and lyophilized to yield OL/PDDA and OL/CH intermediates, respectively.

Procedure for the Loading of Tyrosinase. The reactivity of tyrosinase toward lignin is reported.[42] As a general trend, tyrosinase showed negligible activity toward lignin modification.[48] Tyrosinase from *Aspergillus niger* (1.0 mg, 900 U/mg) was added to a suspension of OL-PDDA (100 mg), or in alternative, to OL/CH (100 mg), in the appropriate buffer (100 mL) under orbital shaking for 24 h at 25 °C. OL/PDDA/tyrosinase (**I**) and OL/CH/tyrosinase (**II**) were recovered by centrifugation (20 min at 6000 rpm). Compounds (**I**) and (**II**) were washed several times with PBS in order to ensure the complete removal of the unbound enzyme (as evaluated by the Bradford method). The recovered solution was used for the evaluation of the activity parameters.

Procedure for the Loading of Laccase. Laccase from *Trametes versicolor* (20 mg, 1.07 U/mg) was added to a suspension of OL-PDDA (100 mg), or in alternative, to OL/CH, in Na-acetate buffer (100 mL) under orbital shaking for 24 h at 25 °C. OL/PDDA/laccase (**III**) and OL/CH/laccase (**IV**) were recovered by centrifugation (20 min at 6000 rpm). Compounds (**III**) and (**IV**) were washed several times with Na-acetate buffer in order to ensure the complete removal of the unbound enzyme (as evaluated by the Bradford method). The recovered solution was used for the evaluation of the activity parameters.

Determination of the Kinetic Parameters. Kinetic parameters of compounds (**I**) and (**II**) (K_m, V_{max}, and V_{max}/K_m) were determined spectrophotometrically by measuring the activity of immobilized tyrosinase at different concentrations of L-tyrosine (0.33−0.10 mM) using the dopachrome method. As a general procedure, the reaction was started by adding L-tyrosine to PBS solution (0.1 M, pH 7) containing the appropriate amount of compounds (**I**) and (**II**) (0.1 mg). The initial rates were measured in a 3.0 mL reaction cuvette as linear increase of the optical density (475 nm) at 25 °C under magnetic stirring.

Kinetic parameters of compounds (**III**) and (**IV**) were determined by measuring the activity of immobilized laccase at different concentrations of ABTS (0.1−5 mM). Briefly, the reaction was started by adding ABTS to compounds (**III**) and (**IV**) (0.1 mg) in Na-acetate solution (0.1 M pH 5). The initial rates were measured in a 3.0 mL reaction cuvette as the linear increase of the optical density at 436 nm at 25 °C under magnetic stirring. The data were analyzed by a double reciprocal Lineweaver−Burk plot. Spectrophotometric data were obtained by using a Cary WinUV (AGILENT, Santa Clara, CA, USA). All experiments were conducted in triplicate using free and immobilized tyrosinase and laccase.

Determination of Activity Parameters. The activity parameters of tyrosinase were determined by measuring the tyrosinase catalyzed oxidation of L-tyrosine by the dopachrome method. As a general procedure, the reaction was started by adding L-tyrosine (0.83 mM) to PBS solution (67 mM, pH 7) containing the appropriate amount (from 45 to 100 units) of samples (**I** and **II**) (from 0.045 to 0.1 mg). The initial rates were measured in a 3.0 mL reaction cuvette as the linear increase of the optical density (475 nm) at 25 °C under magnetic stirring. One unit of enzyme activity was defined as the increase in absorbance of 0.001 unit per minute at pH 7 and 25 °C. Spectrophotometric data were analyzed with Cary WinUV. All experiments were conducted in triplicate. The activity parameters of samples (**III** and **IV**) were assayed by using the ABTS procedure. ABTS (5 mM), sodium acetate buffer (2.0 mL, pH 5.0), and the sample solution (200 μL) were used as the standard solution. The formation of the cation radical was detected by measuring the increase of absorbance at 436 nm. One unit of laccase activity has been defined as the amount of enzyme that catalyzed the oxidation of 1.0 μmol of ABTS in 200 μL of reaction mixture at 25 °C during 1.0 min.

Dynamic Light Scattering. Measurements of particle size and zeta potential were performed on freshly prepared aqueous suspensions (pH = 7) of OL nanocapsules and compounds (**I**) and (**II**) were dispersed in water by dynamic light scattering (DLS) using a Zetasizer Nano ZS (Malvern Instruments, Malvern, UK) apparatus, equipped with an He−Ne laser (633 nm, fixed scattering angle of 173°, 25 °C). Prior to performing size measurements, the suspensions were filtered with a 0.45 μm filter membrane. Measurements were performed in triplicate at room temperature (T = 25 °C).

Procedure for the Pigmentation of Lignin Nanocapsules Functionalized with Tyrosinase. As a general procedure, OL/CH/tyrosinase (**II**) (1.0 mg/mL) was suspended in PBS buffer (pH 7, 0.1 M) in the presence of L-DOPA PBS solution (2 mM), and the suspension was stirred for 2 h at 25 °C under oxygen atmosphere. The black suspension was centrifuged (6000 rpm, 20 min), and the supernatant was removed. Nanocapsules were rinsed three times with KOH (1.0 M) in order to ensure the complete removal of unbound melanin, followed by washing with deionized water up to neutral pH. Next, nanocapsules were recovered by centrifugation (6000 rpm, 20 min) and lyophilized to yield compound (**V**). The amount of unbound melanin in the KOH solution was evaluated spectrophotometrically by comparing the OD at 470 nm of an unknown sample with a standard melanin (1 mg/mL).[49] All measurements were done in triplicate. The disappearance of L-DOPA during the reaction was monitored by gas-chromatography associated with mass-spectrometry (GC−MS). The analyses were performed by a 450 GC-320 MS apparatus using a VF-5MS column and an isothermal temperature profile of 100 °C for 2 min, followed by a 10 °C/min temperature

DOI: 10.1021/acs.biomac.9b00198
Biomacromolecules XXXX, XXX, XXX−XXX

Scheme 1. Structure Model of Lignin[54] and Schematic Preparation of Functionalized Lignin Nanocapsules Supporting Tyrosinase and Laccase[a]

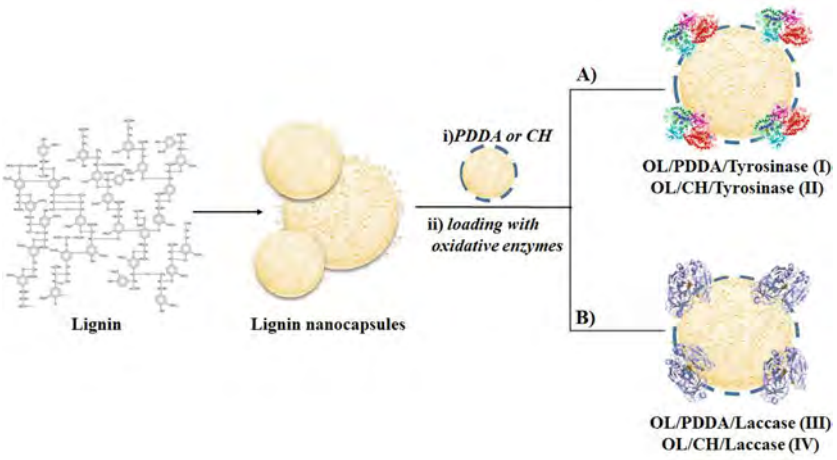

[a]PDDA and CH were used as positively charged polyelectrolytes. Tyrosinase from *Aspergillus niger* and laccase from *Trametes versicolor* are negatively charged at the operative pH. The consecutive deposition of alternatively charged polyelectrolytes was performed on the surface of OL nanocapsules.

gradient to 280 °C for 25 min. The injector temperature was 280 °C. Chromatography-grade helium was used as the carrier gas with a flow of 2.7 mL/min. Mass spectra were recorded with an electron beam of 70 eV.

Procedure for the Pigmentation of Lignin Nanocapsules Functionalized with Laccase. As a general procedure, OL/CH/Laccase (**IV**) (1.0 mg/mL) was suspended in Na-acetate buffer (pH 5, 0.1M) in the presence of the appropriate substrate (2.0 mM) in 0.1 M sodium-acetate buffer (pH 5.0), containing 2% (*v*/*v*) absolute ethanol.[45] The suspension was stirred for 24 h at 25 °C under oxygen atmosphere. The final suspension was centrifuged (6000 rpm, 20 min), and the supernatant was removed. The product was rinsed three times with Milli-Q water (10 mL) in order to ensure the complete removal of unbound pigment. Residual traces of unreacted substrate were monitored by GC−MS. Irrespective to experimental conditions, the quantitative conversion of the substrate was observed.

The colored nanocapsules were recovered by centrifugation (6000 rpm, 20 min) and lyophilized to yield compounds (**VIII**), (**IXa**), (**IXb**), (**Xa**), (**Xb**), (**XIa**), and (**XIb**). The formation of the epicatechin polymer with OL/CH/laccase (**IV**) was evaluated spectrophotometrically in the range of 250−300 nm at different reaction times (1, 2, and 6 h) using the epicatechin monomer as the standard.

Electron Microscopy Analysis. For scanning electron microscopy (SEM), compounds (**V**−**VIII**), (**IXa**), (**IXb**), (**Xa**), (**Xb**), (**XIa**), and (**XIb**) were fixed with 3% glutaraldehyde in 0.1 M cacodylate buffer (pH 7.2) and washed and postfixed in OsO_4 (1% weight) in the same buffer at room temperature. Specimens were dehydrated in a graded ethanol series. They were then air-dried and sputter-coated with gold in a Balzers MED 010 unit. The observation was made by a JEOL JSM 6010LA electron microscope. For transmission electron microscopy (TEM), nanocapsules were placed on Formvar−carbon-coated grids and allowed to be adsorbed for 60 s. Excess liquid was gently removed from each droplet with a strip of filter paper. Processing for negative staining was carried out by placing a drop of negative stain (2%uranyl acetate in distilled water) on the specimen grids, followed by quick blotting. This step was repeated a second time on a new drop of negative staining solution and prolonged for 60 s. Nanocapsules were observed with a JEOL 1200 EX II electron microscope. Micrographs were acquired by the Olympus SIS VELETA CCD camera equipped with the iTEM software.

FTIR Characterization. Attenuated total reflection infrared (ATR-IR) spectroscopic analyses were performed, at room temperature, with a Perkin−Elmer Spectrum One spectrometer equipped with an ATR-IR cell. IR spectra were recorded by averaging 32 scans, with a resolution of 4 cm^{-1}.

EPR Analysis. EPR spectra of solid samples were recorded in a CW (continuous wave) X-band (9 GHz) at room temperature with a Bruker E580 Elexsys Series using the Bruker ER4122SHQE cavity. The 1 mm diameter quartz capillaries were filled in with the samples, and they were placed into a Suprasil tube with a 3.5 mm internal diameter. Experimental conditions for acquisition were 9.87 GHz microwave frequency, 0.1 mT modulation amplitude, and 2 mW microwave power.

Characterization of Color Parameters after Pigmentation of Lignin Nanocapsules. Color parameters were measured through X-Rite CA22 reflectance spectrophotometer according to the CIE $L^*a^*b^*$ color system (ISO 11664-4).[50] In this system, the coordinate L^* describes the lightness, while the coordinates a^* and b^* describe the chromatic coordinates on the green−red and blue−yellow axes, respectively. The characteristics of the color measuring instrument are the following, light source, D65; standard observer, 10°; fixed geometry of measurement, 45°/0°; spectral range, 400−700 nm; spectral resolution, 10 nm; and aperture size, 4 mm. For each sample, three measurements were performed, and then average values and standard deviations were calculated. Data are reported as L^*, a^*, b^*, and reflectance spectra in the visible range.

Effect of Alkaline Treatment and of Ultraviolet Photoirradiation on the Color Strength and Fastness Properties. The effect of UV irradiation on the color change of compounds (**V**) and (**VIII**) in lyophilized powder (60 mg) on a glass slide (size 25 mm × 75 mm) support was performed by UVA and UVB light irradiation, which was provided by UV LAMP 300 W (ULTRA-VITALUX, UVA power 13.6 W and UVB power 3.0 W). After 2 or 24 h of light irradiation, the compounds (**V**) and (**VIII**) were collected for the characterization of color parameters using the untreated compounds as a reference.

As reported in the literature, the effect of the treatment with NaOH (1.0 M) on the color change of compound (**V**) was performed by using a slightly modified procedure.[51] After 2 or 24 h of NaOH (1.0 M) treatment, the final suspension was centrifuged (6000 rpm, 20 min), and the supernatant was removed. The compound (**V**) was lyophilized for the characterization of color parameters using the untreated compound **V** as a reference.

RESULTS AND DISCUSSION

Preparation of Lignin Nanocapsules and Their Loading with Tyrosinase and Laccase. Functionalized

DOI: 10.1021/acs.biomac.9b00198
Biomacromolecules XXXX, XXX, XXX−XXX

Table 1. Kinetic Parameters of Functionalized Lignin Nanocapsules (I)−(IV)

entry	sample	K_m (mM)	$V_{max} \times 10^{-3}$[c] (ΔAbs min μg enzyme)	$V_{max}/K_m \times 10^{-3}$	immobilization yield (%)[d]
1	(I)[a]	0.37	3.89	10.51	90.0
2	(II)[a]	0.36	3.88	10.77	89.5
3	(III)[b]	0.17	1245	7323	64.1
4	(IV)[b]	0.16	1240	7750	62.3

[a]Tyrosinase-based system. L-Tyrosine was used as a substrate. [b]Laccase-based system. ABTS was used as a substrate. [c]V_{max} represents the maximum rate achieved by the system, at a saturating substrate concentration. The Michaelis constant K_m is the substrate concentration at which the reaction rate is half of V_{max}. All experiments were conducted in triplicate. Average errors in kinetic parameters were 2−4% for K_m, and 1−3% for V_{max}. [d]Immobilization yield (%) = $[(U_a - U_r)/U_a] \times 100$. U_a is the total activity (units) of the enzyme added to the solution, and U_r is the residual activity (units) in the washing solutions.

lignin nanocapsules supporting tyrosinase and laccase have been prepared by a modified version of the LbL procedure (Scheme 1, pathway A), consisting of the consecutive deposition of alternatively charged polyelectrolytes onto the appropriate support.[52] The coating protects the enzyme from denaturing agents and allows for regulation of the permeability toward small substrates.[53] Briefly, nanocapsules of OL were obtained by dialysis of a lignin THF solution against deionized water.[46] The OL nanocapsules were used as a template for the sequential deposition of positively charged poly(diallyl dimethylammonium chloride) (PDDA) and negatively charged tyrosinase from *Aspergillus niger*. Kinetic parameters of OL/PDDA/tyrosinase (**I**) (K_m, V_{max}, and V_{max}/K_m), determined by measuring the enzyme activity at different concentrations of L-tyrosine, were found to be in agreement with data previously reported[42] (Table 1, entry 1), confirming the effective loading of the enzyme.

CH, a linear polysaccharide composed of randomly distributed β-(1,4)-D-glucosamine and *N*-acetyl-D-glucosamine units, was successfully used as biodegradable, and there was no toxic alternative to PDDA[55] to yield OL/CH/tyrosinase (**II**). As reported in Table 1 (entry 2), the kinetic parameters of OL/CH/tyrosinase (**II**) were of the same order of magnitude than that of OL/PDDA/tyrosinase (**I**).

The SEM image of compound (**II**) showed nanoparticles with a regular spherical shape and an average diameter of 0.22 ± 0.02 μm (Figure 1). The SEM image of compound (**I**) is reported in the Supporting Information, SI #1. DLS analysis of compounds (**I**) and (**II**) is reported in Figure 2.

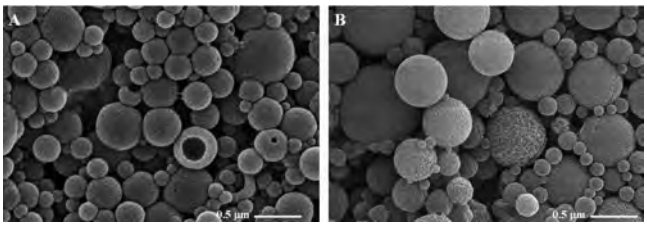

Figure 1. SEM images of lignin nanocapsules. (A) OL nanocapsules. (B) OL/CH/tyrosinase (**II**).

In order to improve the range of catalytic activity, laccase from *Trametes versicolor* was used instead of tyrosinase as a negative layer to yield OL/PDDA/laccase (**III**) and OL/CH/laccase (**IV**), respectively (Scheme 1, pathway B). Kinetic parameters of compounds (**III**) and (**IV**) are reported in Table 1 (entries 3 and 4). Compounds (**III**) and (**IV**) showed kinetic parameters higher than that measured for similar catalysts previously produced by LbL immobilization of laccase on multiwalled carbon nanotubes (MWCNTs).[53] SEM images of

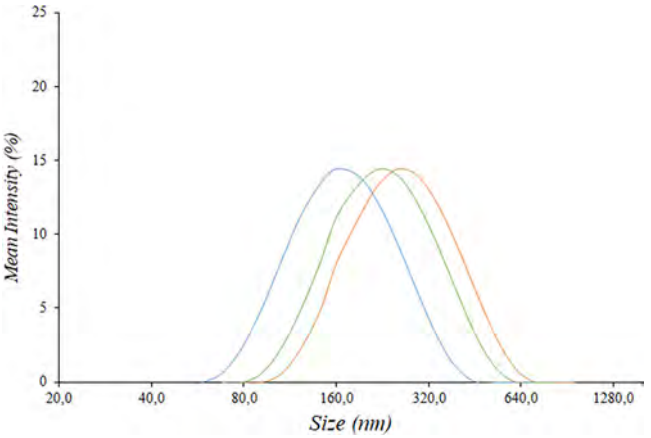

Figure 2. Size distribution and polydispersity index (PDI) of OL nanocapsules (blue line, PDI = 0.349), compound (**I**) (red line, PDI = 0.353), and compound (**II**) (orange line, PDI = 0.382).

compounds (**III**) and (**IV**) are in SI #2. The immobilization yield of samples (**I**)−(**IV**) was evaluated as reported in the following eq (Table 1)

$$\text{Immobilization yield}(\%) = [(U_a - U_r)/U_a] \times 100$$

where U_a is the total activity (units) of the enzyme added to the solution, and U_r is the residual activity (units) in the washing solutions.

Procedure for the Pigmentation of Lignin Nanocapsules Functionalized with Tyrosinase. Tyrosinase (EC 1.14.18.1) catalyzes the conversion of L-tyrosine and L-DOPA to melanin,[56] which is a black pigment widely used in bioink formulations.[57] The mechanism for the synthesis of melanin, especially for the most common variant, eumelanin, is reviewed.[58] It comprises the formation of colored reactive intermediates, such as dopachrome, followed by sequential oxidative coupling reactions.

Eumelanin is usually represented as a complex structure with oligomeric chain lengths of up to a few tenths of monomers and variable chemical composition.[59] Synthetic melanin is mostly reported as amorphous solid without distinctive particles,[60] although some evidence exists that spherical particles can be produced from synthetic sources under controlled conditions.[61] In this latter case, a 3-fold aggregation of oligomers, based on π-stacking interactions, has been proposed.[62]

With the aim to synthesize melanin on the surface of lignin nanocapsules, we decided to use OL/CH/tyrosinase (**II**) as a representative sample, being that this nanodevice was composed of biobased ingredients. OL/CH/tyrosinase (**II**) (1.0 mg/mL) was suspended in PBS buffer (pH 7, 0.1 M) in

DOI: 10.1021/acs.biomac.9b00198
Biomacromolecules XXXX, XXX, XXX−XXX

Scheme 2. Schematic Representation of the Synthesis and Subsequent Deposition of Melanin in the Reaction of OL/CH/Tyrosinase (II) with L-DOPA and L-DOPA/L-Tyrosine Mixtures, Respectively[a]

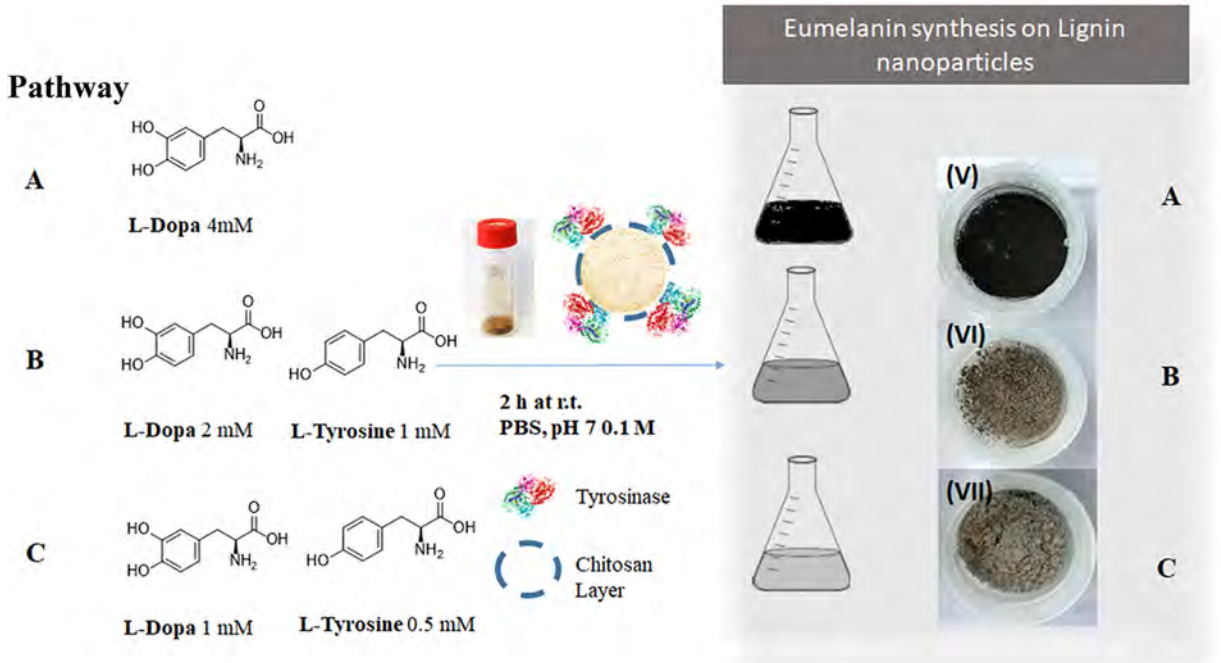

[a]Different shades of gray were obtained depending on the L-DOPA/L-tyrosine ratio.

the presence of L-DOPA (10 mg), and the suspension was stirred at 25 °C under oxygen atmosphere. The system showed a red coloration, probably due to the formation of the dopachrome intermediate, followed by the appearance of the characteristic black coloration of melanin. L-DOPA was completely converted after 2.0 h of reaction time (as evaluated by gas chromatography associated with mass spectroscopy analysis) to yield black lignin nanocapsules (**V**). Nanocapsules (**V**) retained the black coloration after treatment with KOH (1.0 M, 3 × 1.0 mL), suggesting a stable linkage between newly synthesized melanin and the lignin support (Scheme 2, pathway A). Lignin nanocapsules were stable during the KOH treatment, in accordance with previously reported data on the increased stability of lignin nanoparticles at a high pH value, as a consequence of the structuring process.[63] Moreover, the alkaline stability of lignin nanoparticles was found to be significantly improved after chemical grafting with dopamine, due to cross-linking reticulation reactions.[64] Tyrosinase catalyzes the oxidative coupling between phenolic units (even when sterically hindered) by formation of reactive quinone intermediates,[65] which can diffuse toward the chitin layer to the lignin in accordance with the results previously reported on the diffusion- and reaction rate-limited redox processes mediated by quinones through bilayer lipid membranes.[66]

This reaction mechanism might be responsible for the formation of covalent bonds between the phenolic units of lignin and the growing melanin oligomers, assuring the observed stability of the black pigment on the surface of compound (**V**). π-Stacking interactions between the aromatic moieties of the lignin and melanin may be also responsible for the stability of the nanodevice.[62]

TEM and SEM investigations of compound (**V**) (Figures 3 and 4, respectively) showed the deposition of distinguishable

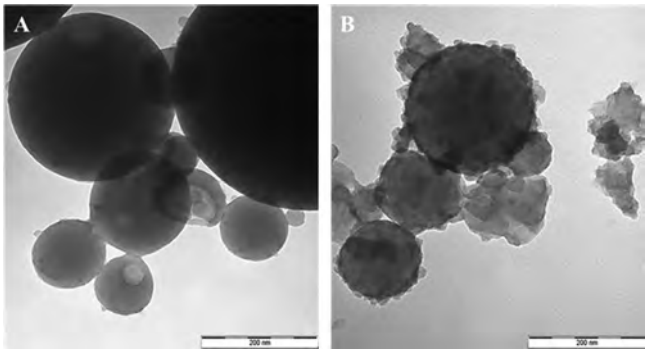

Figure 3. TEM images of lignin nanocapsules. (A) OL nanocapsules. (B) Black lignin nanocapsules (**V**). Agglomerates of amorphous melanin are clearly evident on the surface of lignin.

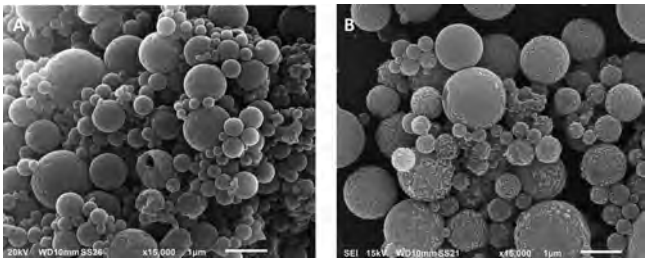

Figure 4. SEM images of lignin nanocapsules. (A) OL nanocapsules. (B) Black lignin nanocapsules (**V**).

agglomerates of melanin on the surface of lignin. The irregular shape of these agglomerates, as highlighted by the TEM analysis, suggested the presence of a variable number of superimposed layers of amorphous melanin. Note, that spherical nanoparticles of melanin have been previously

DOI: 10.1021/acs.biomac.9b00198
Biomacromolecules XXXX, XXX, XXX−XXX

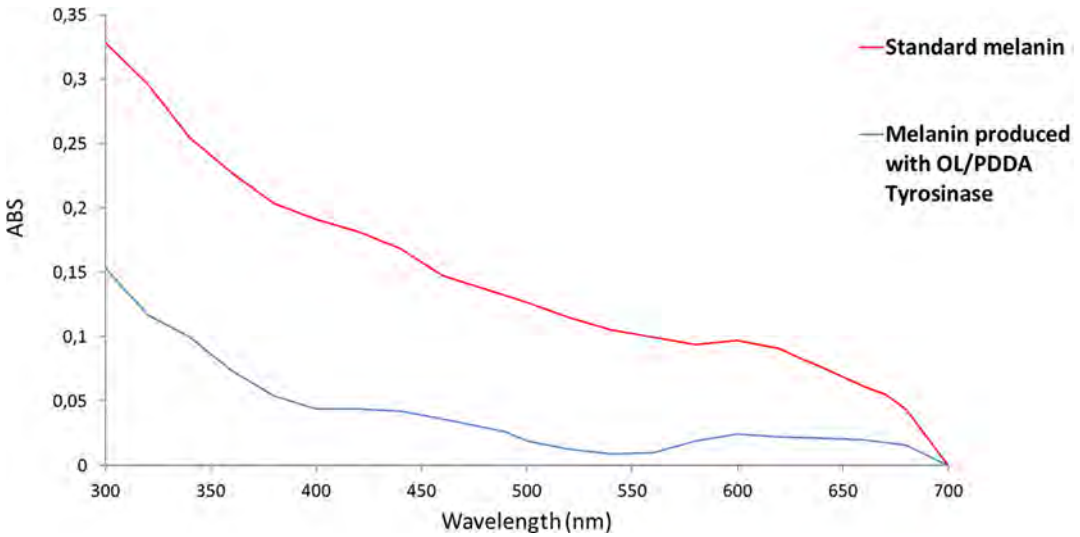

Figure 5. Comparison betweenthe UV−vis spectra of the KOH solution recovered during the preparation of compound (**V**) and the standard sample. (Blue line) UV−vis spectra of unbound melanin produced by polymerization of L-DOPA in the presence of OL/PDDA/tyrosinase (**II**). (Red line) UV−vis spectra of standard melanin.

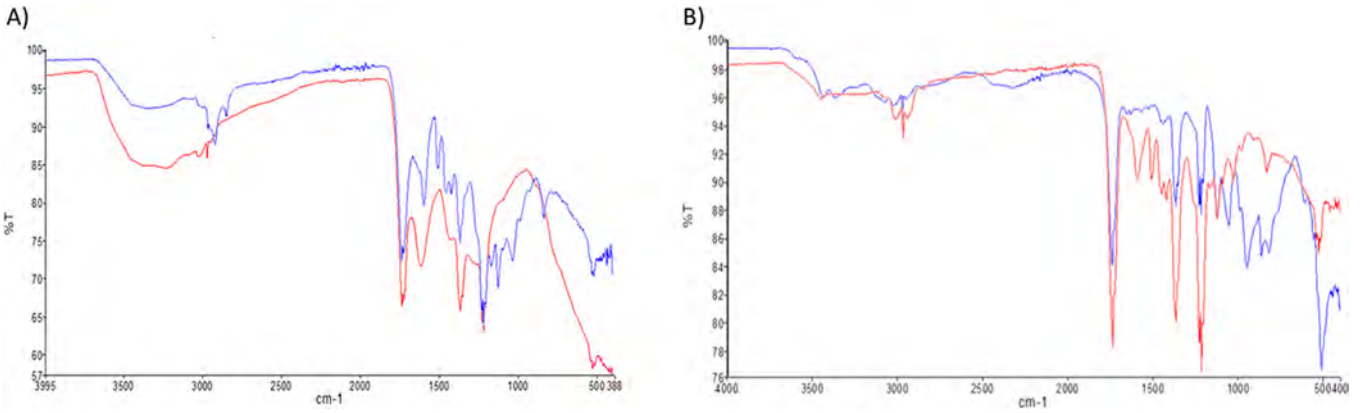

Figure 6. (A) ATR-FTIR spectra of melanin recovered from the KOH solution (blue line) and standard melanin (red line). Band assignment: 3196 cm^{-1}, OH−, NH−, and water (broad signal); 1700 cm^{-1}, quinone (C═O stretching); 1606 cm^{-1}, indole (ring vibration); 1440 cm^{-1}, pyrrole (C═C stretching); 1250 cm^{-1}, pyrrole (N−C stretching); and 1038 cm^{-1}, COOH pyrrole (DHICA monomer). (B) ATR-FTIR spectra of OL/PDDA/tyrosinase (**II**) (red line) and compound (**V**) (blue line). The band at 1038 cm^{-1} COOH in compound (**V**), corresponding to the pyrrole group (DHICA monomer), is a characteristic of the melanin structure.

obtained using tyrosinase adsorbed on an inert glass surface, in which case, interactions were not operative between melanin and the support.[67]

Moreover, the internal spherical shape of compound (**V**) was similar to that of compound (**II**), indicating that the L-DOPA polymerization process was limited to the surface of lignin (Figure 3, panel A versus panel B).

Characterization of the Melanin Pigment and Production of the Gray Color. The UV−vis spectra of the KOH solution recovered during the preparation of compound (**V**) was similar to that of the standard (Figure 5), confirming the synthesis of the melanin pigment. The amount of unbound melanin was measured by comparing the OD at 470 nm with respect to the standard sample.[35] As reported in SI #3, 0.2 mg/mL of unbound melanin was detected, indicating that c.a. 0.8 mg of melanin was retained per 10 mg of compound (**V**).

The ATR-FTIR spectra of compound (**II**) showed the vibration bands for the most frequent monomeric subunits in melanin, 5,6-dihydroxyindole (DHI), and 5,6-dihydroxyindole-2-carboxylic acid (DHICA), respectively. However, the signal of the carboxylic acid (COOH, 1038 cm^{-1}) was not found in the standard, indicating a lower DHICA content in the reference sample of melanin (Figure 6A).

The vibrational bands of melanin were also detected in the ATR-FTIR spectrum of compound (**V**) (Figure 6B), showing the characteristic COOH absorption band associated to the pyrrole group (DHICA monomer) at 1038 cm^{-1}.

The presence of the melanin pigment in sample (**II**) was definitely proven by first-derivative electron paramagnetic resonance (EPR) analysis (Figure 7, Table 2, entry 2), which showed the characteristic melanin EPR signal at a *g*-factor of 2.0041.[68,69]

Next, experiments using L-DOPA in the presence of different concentrations of L-tyrosine were performed in order to tune the shade of the melanin pigment.[70]

When L-DOPA (2.0 mM) was reacted with L-tyrosine (1.0 mM and 0.5 mM, respectively) in the presence of compound (**II**) under previously reported conditions, lignin nanocapsules (**VI**) and (**VII**), characterized by two different shades of gray, were obtained. The lighter shade of gray was observed in the

DOI: 10.1021/acs.biomac.9b00198
Biomacromolecules XXXX, XXX, XXX−XXX

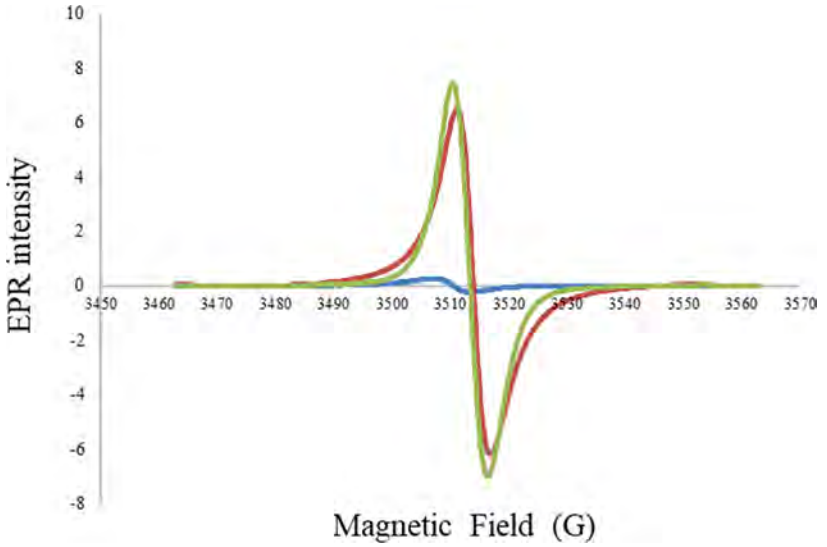

Figure 7. First-derivative EPR analysis of sample (**V**). (Red line) Standard melanin. (Green line) Sample (**V**). (Blue line) OL nanocapsules.

Table 2. Mean Values of *g*-Factor of Samples (V)−(VII)

entry	sample	*g*-factor[a]
1	standard melanin	2.0036
2	(**V**)	2.0041
3	(**VI**)	2.0042
4	(**VII**)	2.0038

[a]The error on the *g*-factors was ±0.0001

presence of the lower amount of L-tyrosine (Scheme 1, pathways B and C), suggesting the possible control of the shade simply by varying the ratio between the reagents. SEM images of nanocapsules (**VI**) and (**VII**) are reported in SI #4.

The effective presence of melanin in compounds (**VI**) and (**VII**) was demonstrated by first-derivative EPR experiments, in which the characteristic signal of melanin was observed at a *g*-factor of 2.0042 and 2.0038, respectively (Table 2, entries 3 and 4). Probably, the gray color was a consequence of a low concentration of the pigment.

Procedure for the Pigmentation of Lignin Nanocapsules Functionalized with Laccase. Laccase (EC 1.10.3.2, *p*-diphenol:dioxygen oxidoreductase) is a multicopper enzyme that catalyzes the oxidation of four molecules of substrate through the direct reduction of dioxygen (O_2).[71] The industrial interest in the application of laccase lies in the low substrate selectivity, high value of catalytic constants, and high

Scheme 3. Schematic Representation of the Synthesis and Subsequent Deposition of Pigments during the Reaction of OL/CH/Laccase (IV) with Phenol Derivatives

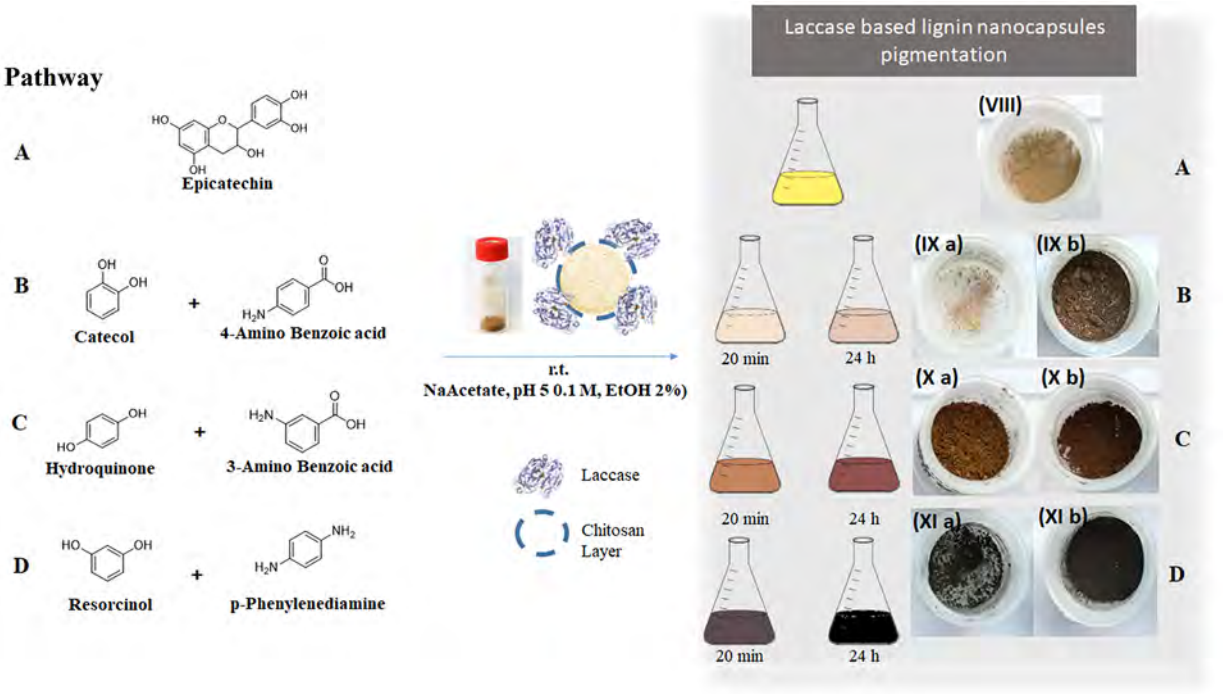

DOI: 10.1021/acs.biomac.9b00198
Biomacromolecules XXXX, XXX, XXX−XXX

thermal resistance.[72] Immobilized laccase has been also used in the chemistry of lignin.[73] Laccase efficiently catalyzes the polymerization of phenol derivatives to form pigments in dying processes and formulations.[45] In this latter case, a large panel of color and a wide range of shade have been obtained by using heteropolymer synthesis.[74] For example, a mixture of natural compounds belonging to the flavonoids family has been successfully applied to give rise to yellow, orange, and dark brown-colored heteropolymers.[75]

When the flavonoid epicathechin (2.0 mM) was treated with OL/CH/laccase (**IV**) (1.0 mg/mL) in Na-acetate buffer (0.1 M, pH 5) at room temperature under dioxygen atmosphere, the yellow-like-colored lignin nanocapsules (**VIII**) were obtained (Scheme 3, pathway A). The color was retained after being washed with Na-acetate buffer, suggesting the occurrence of stable interactions between the epicatechin polymer and lignin. This result is in accordance with data previously reported on the laccase-mediated grafting-process of flavonoids on cotton fibers.[76] The mechanism for the laccase-mediated formation of covalent linkages between raw lignin and flavonoids is reviewed, including the formation of C−C and C−O covalent bonds.[77]

The SEM image of compound (**VIII**) showed spherical capsules with an average diameter of 0.33 ± 0.02 μm (Figure 8A), while in the TEM analysis, the presence of the epicatechin layer surrounding the lignin capsule was highlighted (Figure 8B).

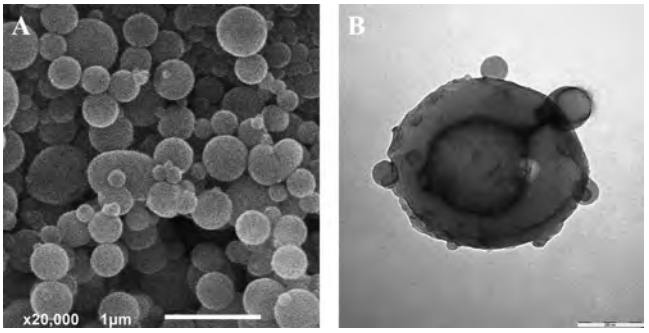

Figure 8. (A) SEM image of the yellow-like lignin nanocapsules (**VIII**). (B) TEM image of the yellow-like lignin nanocapsules (**VIII**).

The formation of the epicatechin polymer was monitored by UV−visible titration at different reaction times (Figure 9). Epicatechin showed a major absorption band in the range of 250−300 nm. The addition of OL/CH/laccase (**IV**) afforded the decrease of the initial absorption band, with the contemporary formation of a new peak in the 325−800 nm range (with a maxima at 392 nm), corresponding to the expected epicatechin polymer.

The ATR-FTIR spectra of compound (**VIII**) confirmed the modification of lignin during the reaction with epicatechin, as evidenced by the disappearance and attenuation of some of the main absorption bands characteristic of lignin (1738, 1364, and 1217 cm^{-1}) (Figure 10A). Moreover, the spectra showed the expected absorption bands, including the OH stretching (3400−3100 cm^{-1}), C═C stretching (1600 cm^{-1}), and C−O stretching (1150−1010 cm^{-1}).[78]

A larger panel of colors was obtained by the reaction of compound (**IV**) with mixtures of phenol derivatives. The treatment of catechol (1.0 mM) and 4-amino-benzoic acid (0.5 mM) with compound (**IV**) afforded pink-like-colored lignin nanocapsules (**IXa** and **IXb**), whose shade intensity was found to be dependent upon reaction time, with the darker shade corresponding to the higher value of reaction time (Scheme 2, pathway B). The presence of catechol/4-amino-benzoic acid heteropolymer on the lignin surface of nanocapsules (**IXa**) was confirmed by the TEM analysis (Figure 11).

ATR-FTIR spectrum of compound (**IXa**) showed typical signals for the amino-benzoic scaffold associated with the formation of the catechol/4-amino-benzoic acid heteropolymer, including frequency at 760, 860, 1490, 1600, and 1640 cm^{-1}[79] (Figure 10B).

Red/brown-like lignin nanocapsules (**Xa**) and (**Xb**) and gray/black lignin nanocapsules (**XIa**) and (**XIb**) have been obtained by the copolymerization of hydroquinone (1.0 mM) with 3-amino benzoic acid (0.5 mM) (Scheme 2, pathway C) and of resorcinol (1.0 mM) with *para*-phenylenediamine (0.5 mM) (Scheme 2, pathway C), respectively. Again, the darker shade of the color was obtained in the correspondence of the highest reaction time. Pigments were found to be stably linked to lignin, confirming the formation of covalent linkages between the colored heteropolymer and the support. TEM images and ATR-FTIR analyses of compounds (**Xa**) and (**XIa**) are in SI #5 and #6, respectively.

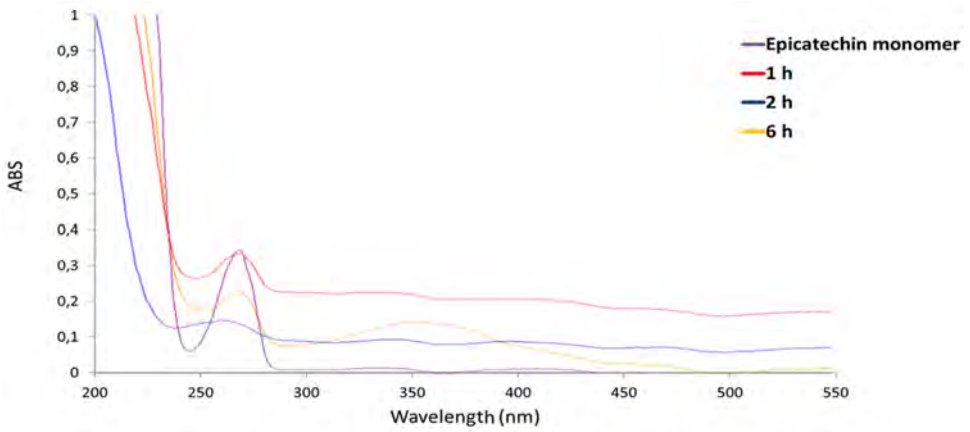

Figure 9. UV−visible titration of the reaction between OL/CH/laccase (**IV**) and epicatechin. Newly synthesized epicatechin polymer showed a characteristic absorption peak in the 325−800 nm range.

DOI: 10.1021/acs.biomac.9b00198
Biomacromolecules XXXX, XXX, XXX−XXX

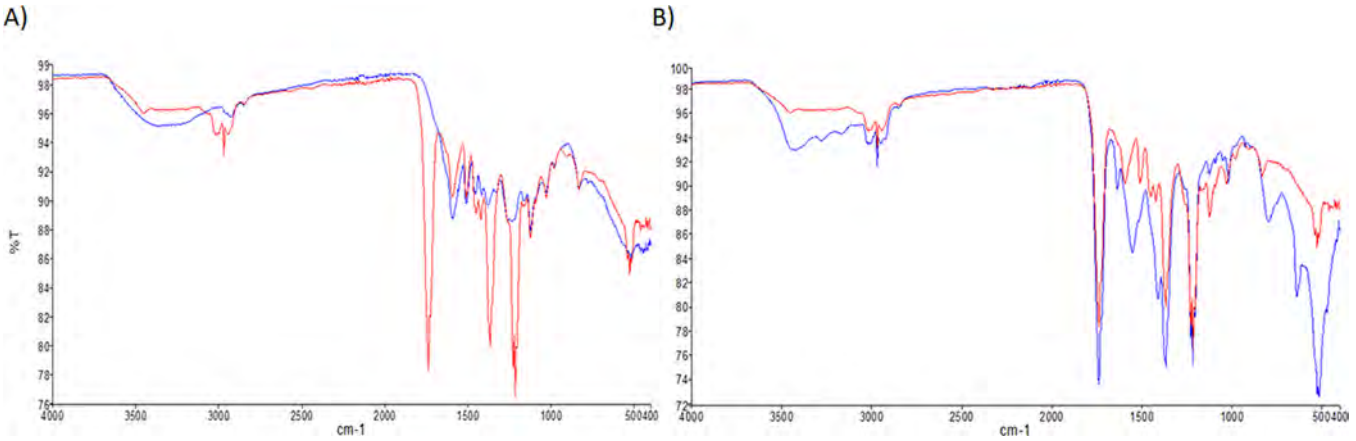

Figure 10. ATR-FTIR spectra of compounds (**VIII**) and (**IXa**). (A, red line) Absorption bands of compound (**IV**). (A, blue line) Absorption bands of compound (**VIII**). (B, red line) Absorption bands of compound (**IV**). (B, blue line) Absorption bands of compound (**IXa**). Characteristic adsorption bands of the amino-benzoic scaffold were found at 760, 860, 1490, 1600, and 1640 cm^{-1}, respectively.

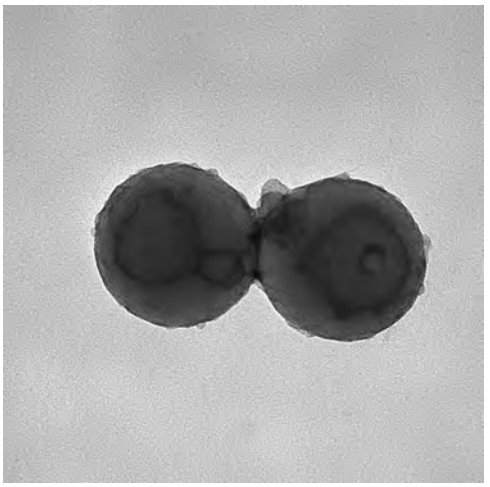

Figure 11. TEM image of nanocapsules (**IXa**).

Unexpectedly, reactions of compound (**IV**) produced also pigments that were unbound to lignin. For example, 2-amino-3-methoxy benzoic acid (Scheme 4, pathway A), 2-methoxy hydroquinone (Scheme 4, pathway B), and the mixture of 4-hydroxy-benzoic acid with ABTS (Scheme 4, pathway C) or, in alternative, the mixture of 4-methylamino benzoic acid with 4-methoxy-phenol (Scheme 4, pathway D) afforded orange, yellow, blue, and violet pigments that were lost during the workup of the reaction.[45]

These data suggested that catechol or hydroquinone moieties were necessary for the formation of a stable linkage between the pigment and lignin. Probably, the higher reactivity of these derivatives with respect to simple phenols in the oxidative cross-coupling process may be responsible for the observed results.[80] This hypothesis is in accordance with the role that quinone derivatives play in the covalent grafting of lignin.[81]

Characterization of Color Parameters after Pigmentation of Lignin Nanocapsules. The characterization of the color parameters of compounds (**V**)−(**VIII**), (**IXa**), (**IXb**), (**Xa**), (**Xb**), (**XIa**), and (**XIb**) has been performed by reflectance spectrophotometry (Figure 12A) using the CIE $L^*a^*b^*$ system (Figures 12B,C). The reflectance spectrum and the values of chromatic coordinates indicated for the reference lignin nanocapsules a yellowish color (average value of b^* equal to 23.3).[82] Compound (**V**) confirmed a black−gray color having low reflectance in the visible spectrum and low values of the chromatic coordinates. A similar trend was observed in compounds (**XIa**) and (**XIb**), that exhibited, in respect to compound (**V**), only a slightly higher value of lightness.

Lignin nanocapsules (**VI**) and (**VII**) showed constant values in the reflectance spectrum along the entire visible range, confirming the light gray color of these samples. The two different gray shades were also documented by color measurements, with compound (**VI**) showing the higher value of lightness and the lower value of b^* with respect to compound (**VII**).

Compound (**VIII**) exhibited a reflectance spectrum similar to that of compounds (**II**) and (**IV**), with a clear dominance of yellow, as showed by the b^* value. Compounds (**IXa**) and (**IXb**) showed a different trend in the reflectance spectra and in the values of chromatic coordinates a^* and b^*; whereas the values of L^* were the same for the two samples. In particular, compound (**IXb**) has a higher value of b^*, indicating a yellow dominance of the color, on the other hand, sample (**IXa**) is located very close to the center of the chromatic diagram, i.e., the gray scale axis.

Compounds (**Xa**) and (**Xb**) exhibited the typical reflectance spectra of orange−red color with a rapid increase of reflectance in the red portion of the visible range at 650−700 nm, especially highlighted in the case of compound (**Xb**).

Effect of Ultraviolet Photoirradiation and Alkaline Treatment on the Color Strength and Fastness Properties. The effect of UV photoirradiation on the color strength and light fastness properties was evaluated in the case of compounds (**V**) and (**VIII**) as representative examples of black-colored and yellow-like-colored nanoparticles. Color strength and light fastness are important physical properties for the quality, weather resistance, and applications of the inks. Alkaline medium and artificial and natural light may cause most pigments to degrade, resulting in color change. The light fastness of inks is important, especially in tattoo, in packaging, and in printing industries.[83] Light fastness refers to the resistance of a color to fading under the sunlight radiation. The effect of UV irradiation on the color change of compounds (**V**) and (**VIII**) is reported in Figure 12D and Table 3. The color changes were defined as both variation of the single chromatic

DOI: 10.1021/acs.biomac.9b00198
Biomacromolecules XXXX, XXX, XXX−XXX

Scheme 4. Unproductive OL/CH/Laccase (IV) Catalyzed Polymerization of Phenol Derivatives 2-Amino-3-methoxy Benzoic Acid (Pathway A), 2-Methoxy Hydroquinone (Pathway B), and of a Mixture of 4-Hydroxy-benzoic Acid with ABTS (Pathway C) or 4-Methyl-amino Benzoic Acid with 4-Methoxy-phenol (Pathway D)[a]

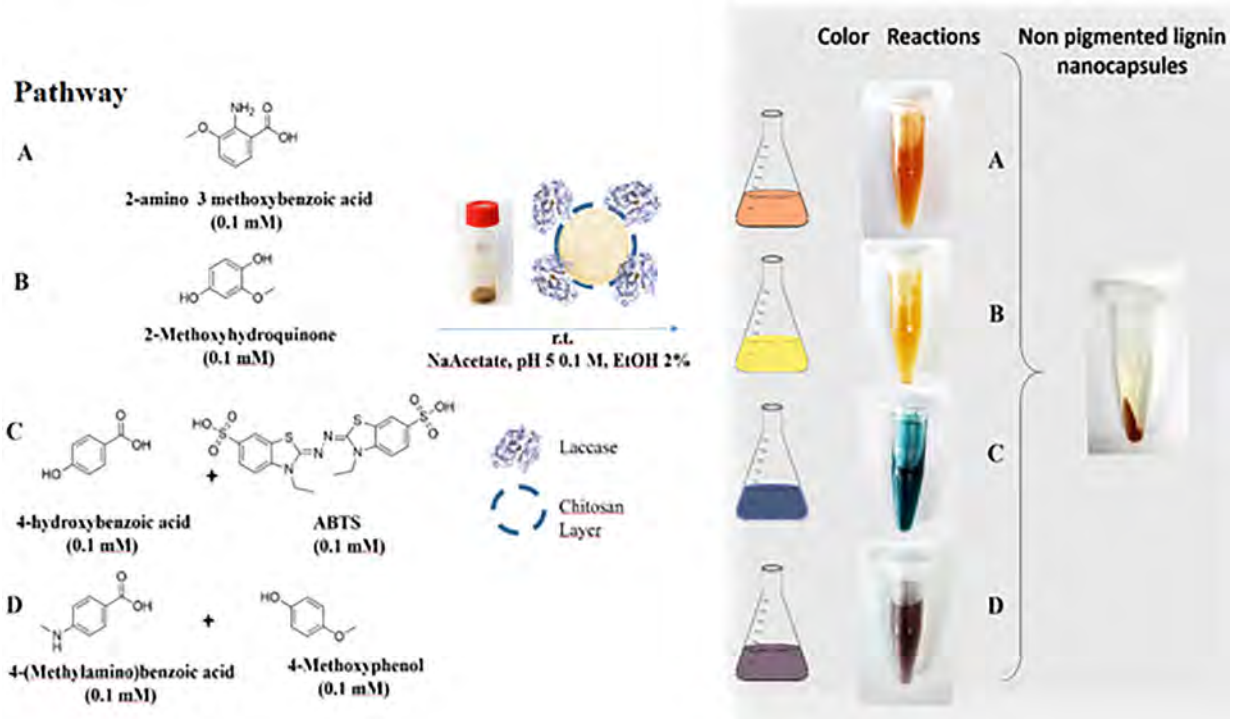

[a]After the reaction, the orange, yellow, blue, and violet pigments were not retained on the surface of the lignin nanocapsules.

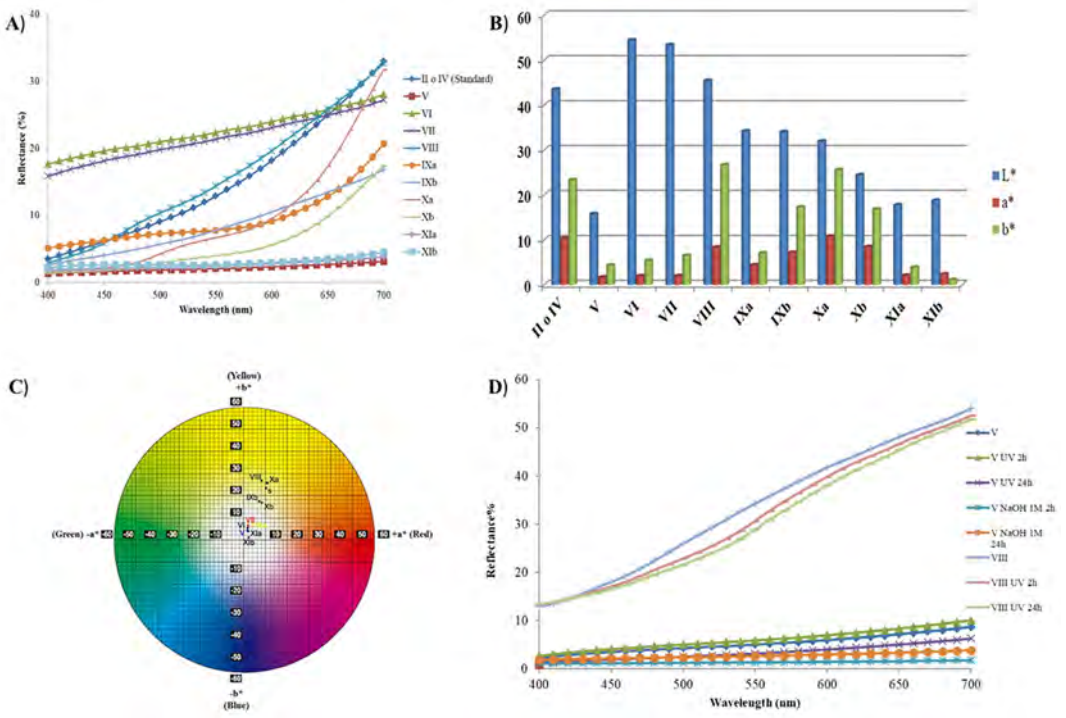

Figure 12. (A) Reflectance spectra of colored lignin nanocapsules (**V**–**VIII**), (**IXa**), (**IXb**), (**Xa**), (**Xb**), (**XIa**), and (**XIb**). (B) CIE $L^*a^*b^*$ parameters of nanocapsules (**V**–**VIII**), (**IXa**), (**IXb**), (**Xa**), (**Xb**), (**XIa**), and (**XIb**). (C) Chromatic diagram for a^*b^* parameters. (D) Reflectance spectra of compound (**V**) and (**VIII**) after UV irradiation and treatment with NaOH.

coordinates and total color variation (ΔE^*). $\Delta E^*$is the geometrical distance between two points in the CIE $L^*a^*b^*$ colorimetric space and is calculated according to eq 1.

$$\Delta E^* = \sqrt{\{(\Delta L^*)^2 + (\Delta a^*)^2 + (\Delta b^*)^2\}} \quad (1)$$

DOI: 10.1021/acs.biomac.9b00198
Biomacromolecules XXXX, XXX, XXX−XXX

Table 3. Variations of the Chromatic Coordinates L^*, a^*, b^*, and Total Color Change (ΔE^*) of Compound (V) and (VIII)

entry	compounds	treatment	L^*[a]	a^*	b^*	ΔL^*	Δa^*	Δb^*	ΔE^*[b]
1	(V)	none	27.2	2.89	8.69				
2	(V)	UV 2 h	29.5	3.04	9.15	2.26	0.15	0.47	2.31
3	(V)	UV 24 h	21.1	4.00	10.0	−6.11	1.11	1.31	6.35
4	(V)	NaOH 1 M 2 h	12.1	0.89	2.08	−15.1	−1.99	−6.61	16.6
5	(V)	NaOH 1 M 24 h	18.7	1.67	4.04	−8.5	−1.22	−4.65	9.77
6	(VIII)	none	65.08	5.98	25.59				
7	(VIII)	UV 2 h	62.78	9.12	23.85	−2.30	3.14	−1.74	4.26
8	(VIII)	UV 24 h	61.41	9.79	22.78	−3.67	3.81	−2.81	5.99

[a] L^* describes the lightness, while a^* and b^* describe the chromatic coordinates on the green-red and blue yellow axes, respectively. [b] ΔE^* is defined as reported in eq 1.

Samples (**V**) and (**VIII**) showed only a slight color variation after 2 h of UV irradiation, as indicated by the ΔE^* value (Table 3, entries 2 and 7). A value of ΔE^* close to 2 is considered imperceptible by human eye, the perceptible variation being observed only at a ΔE^* value close to 5.[84] Interestingly, the sample (**V**) showed a darker black color (that is a decrease of L^*) after 24 h of irradiation (Table 3, entry 3), suggesting the occurrence of a further polymerization process, probably involving semiquinoid-type free radical species, able to increase the π-conjugation degree of the sample.[85] In the case of sample (**VIII**), only a modest ΔE^* variation was observed after 24 h, encompassing the decrease of L^* (darkening), the increase of a^* (reddish trend), and the decrease of b^* (yellowish trend) (Table 3, entry 8).

The treatment of the sample (**V**) with NaOH as the selected example produced a great variation of color after 2 h, mainly due to the change of the L^* value, in association with a slight decrease of b^* (Table 3, entry 4). The resulting color was darker than the reference and completely black, having lost the b^* contribute. The reflectance spectrum further supports this assessment (Figure 12). Note, that a lower value of ΔE^* was observed after 24 h of treatment (Table 3, entry 5). This reaction pattern can be explained assuming that NaOH can initially favor the complete polymerization of melanin quinones intermediates by a general alkaline catalysis,[86] followed by the degradative pathway of lignin for a longer reaction time.[87]

CONCLUSIONS

We have described the preparation of unique and sustainable bioink ingredient-functionalized lignin nanocapsules. The synthesis of the pigment was catalyzed by LbL-immobilized tyrosinase and laccase, with the lignin scaffold performing as the vehicle and binder of the pigment. L-DOPA, L-tyrosine, epicatechin, and other phenol derivatives were used as reactants to afford a large panel of pigments. When tested together, a mixture of phenols afforded different colors, with the specific shade being dependent upon both the reaction time and the ratio between the two reactants. Pigments were found to be stably linked to lignin, suggesting the formation of covalent bonds between the pigment and the support. The presence of the catechol or hydroquinone moiety in the substrate was essential for the stability of the ink. Oxidative coupling processes occurring through reactive quinone intermediates were probably responsible for this effect. The pigmentation process does not modify the spherical shape of lignin nanocapsules, and the pigment was mainly deposited on the surface of lignin, probably in the proximity of immobilized enzymes. Black bioinks characterized by low values of reflectance (samples (**V**), (**XIa**), and (**XIb**)) were obtained. The lowest value of lightness (L^*) was measured for compound (**V**), with it being the blackest ink. Two shades of gray were also obtained (samples (**VI**) and (**VII**)). Yellow shades were observed with compounds (**VIII**), (**IXb**), (**Xa**), and (**Xb**). Lastly, compound (**IXa**) showed a light gray-orange color with low saturation, with it being positioned close to the center of the a*b* chromatic diagram. Compounds (**V**) and (**VIII**) were resistant to ultraviolet photoirradiation. In the case of (**V**), the color darkness increased during the exposition time. Exposure to ultraviolet radiation usually induces the modification of melanin,[88] suggesting the occurrence of a protective effect, probably due to the known UV shielding capacity of lignin at the nanoscale level.[39] Compound (**V**) was also resistant to alkaline treatment, retaining a black coloration darker than the reference, even for prolonged reaction time. The very fact that the pigment is confined on the surface of lignin nanocapsules, which can contemporary act as vehicle, additive, and binder for the pigment, encourages to further evaluate the possibility to use this procedure for the preparation of unique polyvalent bioinks.

ASSOCIATED CONTENT

Supporting Information

The Supporting Information is available free of charge on the ACS Publications website at DOI: 10.1021/acs.biomac.9b00198.

SEM image of compound (**I**), SEM images of compounds (**III**) and (**IV**), melanin concentration after the workup in KOH solution, SEM images of compounds (**VI**) and (**VII**), TEM images of compounds (**Xa**) and compounds (**XI**), and ATR-FTIR analyses of compounds (**Xa**) and (**XIa**) (PDF)

AUTHOR INFORMATION

Corresponding Author

*E-mail: saladino@unitus.it.

ORCID

Bruno Mattia Bizzarri: 0000-0001-7085-5432

Claudia Pelosi: 0000-0002-1338-5267

Raffaele Saladino: 0000-0002-4420-9063

Notes

The authors declare no competing financial interest.

ACKNOWLEDGMENTS

Dr. Maria Camilla Baratto, Department of Biotechnology, Chemistry and Pharmacy, Via A. Moro, 53100 Siena (Italy), is acknowledged for the EPR analysis.

DOI: 10.1021/acs.biomac.9b00198
Biomacromolecules XXXX, XXX, XXX−XXX

REFERENCES

(1) Robert, T. Green ink in all colors'—printing ink from renewable resources. *Prog. Org. Coat.* **2015**, *78*, 287−292.
(2) Leach, R. H. *The printing ink manual*, 5th ed.; Springer: Dordrecht, 2007.
(3) Kipphan, H. *Handbuch der Printmedien*; Springer Verlag: Heidelberg, 2000.
(4) Park, J. M.; Kim, Y. H.; Kim, S. B. Development of Solvent-Free Offset Ink Using Vegetable Oil Esters and High Molecular Weight Resin. *J. Oleo Sci.* **2013**, *62*, 345−352.
(5) Roy, A. S.; Bhattacharjee, M.; Mondal, R.; Ghosh, S. Development of Mineral Oil Free Offset Printing Ink Using Vegetable Oil Esters. *J. Oleo Sci.* **2007**, *56*, 623−628.
(6) Karlberg, A. T. In *Colophony: Rosin in Unmodified and Modified Form. In Occupational Dermatology*; Springer: Berlin, Heidelberg, 2012.
(7) Erhan, S. Z.; Bagby, M. O. Vegetable Oil-based Printing Ink. US Patent US05122188, 1992.
(8) Mello, V. M.; Oliveira, G. V.; Suarez, P.A.Z. J. Turning used frying oil into a new raw material to printing inks. *J. Braz. Chem. Soc.* **2013**, *24*, 314−319.
(9) Bhattacharjee, M.; Roy, A. S.; Ghosh, S.; Dey, M. Development of Karanja Oil Based Offset Printing Ink in Comparison with Linseed Oil. *J. Oleo Sci.* **2011**, *60*, 19−24.
(10) Ha, Y. B.; Jin, M. Y.; Oh, S. S.; Ryu, D. H. Synthesis of an Environmentally Friendly Phenol-Free Resin for Printing Ink. *Bull. Korean Chem. Soc.* **2012**, *33*, 3413−3416.
(11) Shelton, A. M. C.; Posey-Dowty, J. D.; Rios Perdomo, L. G.; Dixon, D. W., Jr.; Lucas, P. L.; Wilson, A. K.; Walker, K. R.; Lawniczak, J. E.; Foulk, R. G.; Phan, H. D.; Freeman, C. C., Jr. Low Molecular Weight Cellulose Mixed Esters and their Use as Low Viscosity Binders and Modifiers in Coating Compositions. US Patent US2011/0282049A1; Eastman Chemical Co., 2011,.
(12) De Meester, A. S.; Callewaert, C.; De Mol, E.; Van Langenhove, H.; Dewulf, J. The resource footprint of biobased products: a key issue in the sustainable development of biorefineries Bio-fuels Bioprod. *Biofuels, Bioprod. Biorefin.* **2011**, *5*, 570−580.
(13) Ragauskas, A. J.; Beckham, G. T.; Biddy, M. J.; Chandra, R.; Chen, F.; Davis, M. F.; Davison, B. H.; et al. Lignin Valorization: Improving Lignin Processing in the Biorefinery. *Science* **2014**, *344*, 1246843−1246843.
(14) Calvo-Flores, F. G.; Dobado, J. A. Lignin as Renewable Raw Material. *ChemSusChem* **2010**, *3*, 1227−1235.
(15) Kaur, R.; Uppal, S. K. Structural characterization and antioxidant activity of lignin from sugarcane bagasse. *Colloid Polym. Sci.* **2015**, *293*, 2585−2592.
(16) Azadfar, M.; Gao, A. H.; Bule, M. V.; Chen, S. Structural characterization of lignin: A potential source of antioxidants guaiacol and 4-vinylguaiacol. *Int. J. Biol. Macromol.* **2015**, *75*, 58−66.
(17) Pan, X.; Kadla, J. F.; Ehara, K.; Gilkes, N.; Saddler, J. N. Organosolv Ethanol Lignin from Hybrid Poplar as a Radical Scavenger: Relationship between Lignin Structure, Extraction Conditions, and Antioxidant Activity. *J. Agric. Food Chem.* **2006**, *54*, 5806−5813.
(18) Ugartondo, V.; Mitjans, M.; Vinardell, M. P. Comparative antioxidant and cytotoxic effects of lignins from different sources. *Bioresour. Technol.* **2008**, *99*, 6683−6687.
(19) Zimniewska, M.; Batog, J.; Bogacz, E.; Romanowska, B. Functionalization of natural fibres textiles by improvement of nanoparticles fixation on their surface. *J. Fiber Bioeng. Inf.* **2018**, *5*, 321−339.
(20) Glasser, W. G. Lignin: Historical, Biological, and Materials Perspectives. In *Classification of Lignin According to Chemical and Molecular Structure*; 1999; pp 216−238.
(21) Qian, Y.; Qiu, X.; Zhu, S. Lignin: a nature-inspired sun blocker for broad-spectrum sunscreens. *Green Chem.* **2015**, *17*, 320−324.
(22) Ding, J.; Gu, L.; Dong, W.; Yu, H. Epoxidation Modification of Renewable Lignin to Improve the Corrosion Performance of Epoxy Coating. *Int. J. Electrochem. Sci.* **2016**, *11*, 6256−6265.
(23) Hussin, M. H.; Shah, A. M.; Rahim, A. A.; Ibrahim, M. N. M.; Perrin, D.; Brosse, N. Antioxidant and anticorrosive properties of oil palm frond lignins extracted with different techniques. *Ann. For. Sci.* **2015**, *72*, 17−26.
(24) Milczarek, G.; Nowicki, M. Carbon nanotubes/kraft lignin composite: Characterization and charge storage properties. *Mater. Res. Bull.* **2013**, *48*, 4032−4038.
(25) Gnedenkov, S. V.; Sinebryukhov, S. L.; Opra, D. P.; Zemnukhova, L. A.; Tsvetnikov, A. K.; Minaev, A. N.; Sergienko, V. I.; Sokolov, A. A. Electrochemistry of Klason Lignin. *Procedia Chem.* **2014**, *11*, 96−100.
(26) Espinoza-Acosta, J. L.; Torres-Chávez, P. I.; Olmedo-Martínez, J. L.; Vega-Rios, A.; Flores-Gallardo, S.; Zaragoza-Contreras, E. A. Lignin in storage and renewable energy applications: A review. *J. Energy Chem.* **2018**, *27*, 1422−1438.
(27) Schilling, P. Lignin Amine Salt-Based Binders for Water-Based Black Ink Formulations. US Patent US05188665; Westvaco Co., 1993.
(28) Belgacem, M. N.; Blayo, A.; Gandini, A. Organosolv lignin as a filler in inks, varnishes and paints. *Ind. Crops Prod.* **2003**, *18*, 145−153.
(29) Finch, C. A. In *Advanced wood adhesives technology*; Pizzi, A., Ed.; Dekker: New York, 1994; Chapter V.
(30) Caes, B.; Rivas, M.; Noirot, P. A. Printing Ink with Nitrates Lignin Ester As binder component. WO 2015/062910 A1, 2015.
(31) Michael, D. Matzinger Water-based ink jet ink compositions containing carboxylated lignin. US Patent US6045606A; Westvaco Co., 1999.
(32) Miller, J. E.; Dilling, P., Jr. Water-based printing ink compositions containing a lignin acetate binder US Patent US4612051A; Westvaco Co., 1985.
(33) Beisl, S.; Friedl, A.; Miltner, A. Lignin from Micro- to Nanosize: Applications. *Int. J. Mol. Sci.* **2017**, *18*, 2367.
(34) Figueiredo, P.; Lintinen, K.; Kiriazis, A.; Hynninen, H.; Liu, Z.; Bauleth-Ramos, T.; Rahikkala, A.; Correia, A.; Kohout, T.; Sarmento, B.; Yli-Kauhaluoma, J.; Hirvonen, J.; Ikkala, O.; Kostiainen, M. A.; Santos, H. A. In vitro evaluation of biodegradable lignin-based nanoparticles for drug delivery and enhanced antiproliferation effect in cancer cells. *Biomaterials* **2017**, *121*, 97−108.
(35) Tian, D.; Hu, J.; Bao, J.; Chandra, R. P.; Saddler, J. N.; Lu, C. Lignin valorization: lignin nanoparticles as high-value bio-additive for multifunctional nanocomposites. *Biotechnol. Biofuels* **2017**, *10*, 192.
(36) Vukoje, M.; Miljanić, S.; Hrenović, J.; Rožić, M. Thermochromic ink−paper interactions and their role in biodegradation of UV curable prints. *Cellulose* **2018**, *25*, 6121−6138.
(37) Schilling, P. Submicron lignin-based binders for water-based black ink formulations. US Patent US005192361A; Westvaco Co., 1992.
(38) Moon, R. J.; Martini, A.; Nairn, J.; Simonsen, J.; Youngblood, J. Cellulose nanomaterials review: structure, properties and nanocomposites. *Chem. Soc. Rev.* **2011**, *40*, 3941−3994.
(39) Piccinino, D.; Capecchi, E.; Botta, L.; Bizzarri, B. M.; Bollella, P.; Antiochia, R.; Saladino, R. Layer-by-Layer Preparation of Microcapsules and Nanocapsules of Mixed Polyphenols with High Antioxidant and UV-Shielding Properties. *Biomacromolecules* **2018**, *19*, 3883−3893.
(40) Ball, V.; Bernsmann, F.; Betscha, C.; Maechling, C.; Kauffmann, S.; Senger, B.; Voegel, J. C.; Schaaf, P.; Benkirane-Jessel, N. Polyelectrolyte multilayer films built from poly(L-lysine) and a two-component anionic polysaccharide blend. *Langmuir* **2009**, *25*, 3593−6000.
(41) Sipponen, M. H.; Farooq, M.; Koivisto, J.; Pellis, A.; Seitsonen, J.; Österberg, M. Spatially confined lignin nanospheres for biocatalytic ester synthesis in aqueous media. *Nat. Commun.* **2018**, *9*, 2300.
(42) Capecchi, E.; Piccinino, D.; Delfino, I.; Bollella, P.; Antiochia, R.; Saladino, R. Functionalized Tyrosinase-Lignin Nanoparticles as Sustainable Catalysts for the Oxidation of Phenols. *Nanomaterials* **2018**, *8*, 438.

DOI: 10.1021/acs.biomac.9b00198
Biomacromolecules XXXX, XXX, XXX−XXX

(43) Frommhagen, M.; Mutte, S. K.; Westphal, A. H.; Koetsier, M. J.; Hinz, S. W. A.; Visser, J.; Kabel, M. A.; et al. Boosting LPMO-driven lignocellulose degradation by polyphenol oxidase-activated lignin building blocks. *Biotechnol. Biofuels* **2017**, *10*, 1.
(44) Shleev, S.; Jarosz-Wilkolazka, A.; Khalunina, A.; Morozova, O.; Yaropolov, A.; Ruzgas, T.; Gorton, L. Direct electron transfer reactions of laccases from different origins on carbon electrodes. *Bioelectrochemistry* **2005**, *67*, 115−124.
(45) Polak, J.; Jarosz-Wilkolazka, A. Structure/Redox potential relationship of simple organic compounds as potential precursors of dyes for laccase-mediated transformation. *Biotechnol. Prog.* **2012**, *28*, 93−102.
(46) Lievonen, M.; Valle-Delgado, J. J.; Mattinen, M.-L.; Hult, E.-L.; Lintinen, K.; Kostiainen, M. A.; Paananen, A.; Szilvay, G. R.; Setälä, H.; Österberg, M. A simple process for lignin nanoparticle preparation. *Green Chem.* **2016**, *18*, 1416−1422.
(47) Jiang, C.; He, H.; Jiang, H.; Ma, L.; Jia, D. M. Nano-lignin filled natural rubber composites: Preparation and characterization. *eXPRESS Polym. Lett.* **2013**, *7*, 480−493.
(48) Grönqvist, S.; Viikari, L.; Niku-Paavola, M. L.; Orlandi, M.; Canevali, C.; Buchert, J. Oxidation of milled wood lignin with laccase, tyrosinase and horseradish peroxidase. *Appl. Microbiol. Biotechnol.* **2005**, *67*, 489−94.
(49) Makpol, S.; Jam, F. A.; Rahim, N. A.; Khor, S. C.; Ismail, Z.; Yusof, Y. A.; Wan Ngah, W. Z. Comparable down-regulation of TYR, TYRP1 and TYRP2 genes and inhibition of melanogenesis by tyrostat, tocotrienol-rich fraction and tocopherol in human skin melanocytes improves skin pigmentation. *Clin. Ter.* **2014**, *165*, 39−45.
(50) ISO 11664-4. Colorimetry - Part 4: CIE 1976 L*a*b* Colour space, 2008.
(51) Mattinen, M. L.; Valle-Delgado, J. J.; Leskinen, T.; Anttila, T.; Riviere, G.; Sipponen, M.; Österberg, M.; et al. Enzymatically and chemically oxidized lignin nanoparticles for biomaterial applications. *Enzyme Microb. Technol.* **2018**, *111*, 48−56.
(52) Decher, G. Fuzzy Nanoassemblies: Toward Layered Polymeric Multicomposites. *Science* **1997**, *277*, 1232−1237.
(53) Piccinino, D.; Delfino, M.; Botta, G.; Crucianelli, M.; Grossi, V.; Passacantando, M.; Saladino, R.; et al. Highly efficient synthesis of aldehydes by layer-by-layer multi-walled carbon nanotubes (MWCNTs) laccase mediator systems. *Appl. Catal., A* **2015**, *499*, 77−88.
(54) Glazer, A. N.; Nikaido, H. In *Microbial Biotechnology: fundamentals of applied microbiology*; W. H. Freeman: San Francisco, 1995; p 340.
(55) Richert, L.; La Valle, P.; Payan, E.; Shu, X. Z.; Prestwich, G. D.; Stoltz, J.-F.; Schaaf, P.; Voegel, J.-C.; Picart, C. Layer by Layer Buildup of Polysaccharide Films: Physical Chemistry and Cellular Adhesion Aspects. *Langmuir* **2004**, *20*, 448−458.
(56) Liu, Y.; Ai, K.; Liu, J.; Deng, M.; He, Y.; Lu, L. Dopamine-melanin colloidal nanospheres: An efficient near-infrared photothermal therapeutic agent for in vivo cancer therapy. *Adv. Mater.* **2013**, *25*, 1353−1359.
(57) Neifar, A.; Ben Abdelmalek, I.; Bouajila, G.; Kolsi, R.; Bradai, M. N.; Abdelmouleh, A.; Gargouri, A.; Ayed, N. Purification and incorporation of the black ink of cuttlefish *Sepia officinalis* in eye cosmetic products. *Color. Technol.* **2013**, *129*, 150−154.
(58) Ito, S. A chemist's view of melanogenesis. *Pigm. Cell Res.* **2003**, *16*, 230−236.
(59) Reale, S.; Crucianelli, M.; Pezzella, A.; d'Ischia, M.; de Angelis, F. Exploring the frontiers of synthetic eumelanin polymers by high-resolution matrix-assisted laser/desorption ionization mass spectrometry. *J. Mass Spectrom.* **2012**, *47*, 49−53.
(60) Nofsinger, J. B.; Forest, S. E.; Eibest, L. M.; Gold, K. A.; Simon, J. D. Probing the Building Blocks of Eumelanins Using Scanning Electron Microscopy. *Pigm. Cell Res.* **2000**, *13*, 179−184.
(61) Kim, D. J.; Ju, K. Y.; Lee, J. K. The Synthetic Melanin Nanoparticles Having An Excellent Binding Capacity of Heavy Metal Ions. *Bull. Korean Chem. Soc.* **2012**, *33*, 3788−3792.
(62) Xiao, M.; Chen, W.; Li, W.; Zhao, J.; Hong, Y.; Nishiyama, Y.; Miyoshi, T.; Shawkey, M. D.; Dhinojwala, A. 2018 Elucidation of the hierarchical structure of natural eumelanins. *J. R. Soc., Interface* **2018**, *15*, 20180045.
(63) Xiong, F.; Han, Y.; Wang, S.; Li, G.; Qin, T.; Chen, Y.; Chu, F. Preparation and Formation Mechanism of Renewable Lignin Hollow Nanospheres with a Single Hole by Self-Assembly. *ACS Sustainable Chem. Eng.* **2017**, *5*, 2273−2281.
(64) Xing, Q.; Buono, P.; Ruch, D.; Dubois, P.; Wu, L.; Wang, W. J. Biodegradable UV-Blocking Films through Core−Shell Lignin−Melanin Nanoparticles in Poly(butylene adipate-co-terephthalate). *ACS Sustainable Chem. Eng.* **2019**, *7*, 4147−4157.
(65) Bizzarri, B. M.; Martini, A.; Serafini, F.; Aversa, D.; Piccinino, D.; Botta, L.; Berretta, N.; Guatteo, E.; Saladino, R. Tyrosinase mediated oxidative functionalization in the synthesis of DOPA-derived peptidomimetics with anti-Parkinson activity. *RSC Adv.* **2017**, *7*, 20502−20509.
(66) Ilani, A.; Krakover, T. Diffusion- and reaction rate-limited redox processes mediated by quinones through bilayer lipid membranes. *Biophys. J.* **1987**, *51*, 161−167.
(67) Strube, O. I.; Büngeler, A.; Bremser, W. Site-Specific In Situ Synthesis of Eumelanin Nanoparticles by an Enzymatic Autodeposition-Like Process. *Biomacromolecules* **2015**, *16*, 1608.
(68) Surwase, S. N.; Patil, S. A.; Jadhav, S. B.; Jadhav, J. P. Optimization of l-DOPA production by Brevundimonas sp. SGJ using response surface methodology. *Microb. Biotechnol.* **2012**, *5*, 731−737.
(69) Al Khatib, M.; Harir, M.; Costa, J.; Baratto, M.; Schiavo, I.; Trabalzini, L.; Pollini, S.; Rossolini, G.; Basosi, R.; Pogni, R. Spectroscopic Characterization of Natural Melanin from a Streptomyces cyaneofuscatus Strain and Comparison with Melanin Enzymatically Synthesized by Tyrosinase and Laccase. *Molecules* **2018**, *23*, 1916.
(70) Robbins, R. In *Chemical and physical behavior of human hair, in Genetic Control/Involvement in Hair Fiber Traits*, 5th ed.; Springer: Berlin, Germany, 2012; Chapter 3, pp 177−203.
(71) Yaropolov, A. I.; Skorobogat'ko, O. V.; Vartanov, S. S.; Varfolomeyev, S. D. Laccase. *Appl. Biochem. Biotechnol.* **1994**, *49*, 257−280.
(72) Riva, S. Laccases: blue enzymes for green chemistry. *Trends Biotechnol.* **2006**, *24*, 219−226.
(73) Crestini, C.; Perazzini, R.; Saladino, R. Oxidative functionalisation of lignin by layer-by-layer immobilised laccases andlaccase microcapsules. *Appl. Catal., A* **2010**, *372*, 115−123.
(74) Jeon, J. R.; Kim, E. J.; Murugesan, K.; Park, H. K.; Kim, Y. M.; Kwon, J. H.; Chang, Y. S.; et al. Laccase-catalysed polymeric dye synthesis from plant-derived phenols for potential application in hair dyeing: Enzymatic colourations driven by homo- or hetero-polymer synthesis. *Microb. Biotechnol.* **2010**, *3*, 324−335.
(75) Song, J. E.; Su, J.; Noro, J.; Cavaco-Paulo, A.; Silva, C.; Kim, H. R. Bio-coloration of bacterial cellulose assisted by immobilized laccase. *AMB Express* **2018**, *8*, 19.
(76) Kim, S.; Moldes, D.; Cavaco-Paulo, A. Laccases for enzymatic colouration of unbleached cotton. *Enzyme Microb. Technol.* **2007**, *40*, 1788−1793.
(77) Slagman, S.; Zuilhof, H.; Franssen, M. C. R. Laccase-Mediated Grafting on Biopolymers and Synthetic Polymers: A Critical Review. *ChemBioChem* **2018**, *19*, 288−311.
(78) Maoela, M. S.; Arotiba, O. A.; Baker, P. G.; Mabusela, W. T.; Jahed, N.; Songa, E. A.; Iwuoha, E. I. Electroanalytical determination of catechin flavonoid in ethyl acetate extracts of medicinal plants. *Int. J. Electrochem. Sci.* **2009**, *4*, 1497−1510.
(79) Lide, D. R.; Milne, G. W. A. In *Handbook of Data on Organic Compounds*, 3rd ed.; CRC Press, Inc.: Boca Raton, FL, 1994; *V2*, p 1348.
(80) Yang, J.; Cohen Stuart, M. A.; Kamperman, M. Jack of All Trades: Versatile Catechol Crosslinking Mechanisms. *Chem. Soc. Rev.* **2014**, *43*, 8271−8298.
(81) Nyanhongo, G. S.; Kudanga, T.; Nugroho Prasetyo, E.; Gübitz, G. M. Enzymatic Polymer Functionalisation: Advances in Laccase and

DOI: 10.1021/acs.biomac.9b00198
Biomacromolecules XXXX, XXX, XXX−XXX

Peroxidase Derived Lignocellulose Functional Polymers. *Adv. Biochem. Eng./Biotechnol.* **2010**, *125*, 47−68.
(82) Ajao, O.; Jeaidi, J.; Benali, M.; Restrepo, A. M.; El Mehdi, N.; Boumghar, Y. Quantification and Variability Analysis of Lignin Optical Properties for Colour-Dependent Industrial Applications. *Molecules* **2018**, *23*, 377.
(83) Aydemir, C.; Yenidogan, S. Light fastness of printing inks: A review. *Journal of Graphic Engineering and Design.* **2018**, *9*, 37−43.
(84) Mokrzycki, W. S.; Tatol, M. Colour difference Δ E-A survey. *Machine Graphics and Vision.* **2011**, *20*, 383−411.
(85) Solano, F. Melanins: Skin Pigments and Much More—Types, Structural Models, Biological Functions, and Formation Routes. *New Journal of Science.* **2014**, *2014*, 1−28.
(86) Ragimov, A. V.; Mamedov, B. V.; Liogonkii, B. The alkali initiated polymerization of p-benzoquinone. *Polym. Sci. U.S.S.R.* **1977**, *19*, 2922−2928.
(87) Erdocia, X.; Prado, R.; Corcuera, M.Á.; Labidi, J. Base catalyzed depolymerization of lignin: Influence of organosolv lignin nature. *Biomass Bioenergy* **2014**, *66*, 379−386.
(88) Ito, S.; Wakamatsu, K.; Sarna, T. Photodegradation of Eumelanin and Pheomelanin and Its Pathophysiological Implications. *Photochem. Photobiol.* **2018**, *94*, 409−420.

DOI: 10.1021/acs.biomac.9b00198
Biomacromolecules XXXX, XXX, XXX−XXX